Carbon Nanotube-Filled Nanofibrous Membranes Electrospun from Poly(acrylonitrile-co-acrylic acid) for Glucose Biosensor

ARTICLE *in* THE JOURNAL OF PHYSICAL CHEMISTRY C · FEBRUARY 2009

Impact Factor: 4.77 · DOI: 10.1021/jp807047s

5 AUTHORS, INCLUDING:

Guang Li
Zhejiang University
101 PUBLICATIONS **1,131** CITATIONS
SEE PROFILE

Zhi-Kang Xu
Zhejiang University
249 PUBLICATIONS **6,251** CITATIONS
SEE PROFILE

Carbon Nanotube-Filled Nanofibrous Membranes Electrospun from Poly(acrylonitrile-*co*-acrylic acid) for Glucose Biosensor

Zhen-Gang Wang,[†] You Wang,[‡] Hui Xu,[‡] Guang Li,[‡] and Zhi-Kang Xu*,[†]

Institute of Polymer Science and Key Laboratory of Macromolecular Synthesis and Functionalization (Ministry of Education), and State Key Laboratory of Industrial Control Technology, Institute of Advanced Process Control, Zhejiang University, Hangzhou 310027, People's Republic of China

Received: August 7, 2008; Revised Manuscript Received: November 10, 2008

Due to its unique electrical properties, carbon nanotubes offer the exciting possibility for developing ultrasensitive electrochemical biosensors. In this work, nanofibrous membranes filled with multiwalled carbon nanotube (MWCNT) were electrospun from the mixture of poly(acrylonitrile-*co*-acrylic acid) (PANCAA) and MWCNT. These nanofibrous membranes were directly deposited on Pt electrodes for the fabrication of glucose biosensors. Glucose oxidase (GOx) was covalently immobilized on the membranes through the activation of carboxyl groups on the PANCAA nanofiber surface. The fluorescence spectra and circular dichroism were recorded from the mixtures of MWCNT and soluble GOx. Results show that MWCNT will disturb the secondary structure of soluble GOx but can get close to its active site. The morphologies of the nanofibrous membranes were visualized by scanning electron microscopy, illustrating that the membranes are composed of beads and nanofibers. The electrochemical properties of enzyme electrodes were characterized by chronoamperometric measurments. It is found that as MWCNT concentration increases, the current enhances correspondingly with a maximum of 50%, while the MWCNT filling delays the electrode response. Kinetic studies of the electrodes show that the secondary structure of the immobilized GOx is disturbed, while the embedded MWCNT enhances the maximum current of GOx electrode. Moreover, the enzyme electrodes can be used up to 6 times with a small decrease in current.

1. Introduction

Electrospinning has proved to be a simple and versatile technique to fabricate continuous fibers with diameters ranging from several micrometers down to a few nanometers.[1,2] Those membranes assembled by electrospun nanofibers are characterized by large surface area-to-volume ratio, high porosity, and interconnectivity. These features provide great potential for the nanofibrous membranes in enzyme immobilization,[3−5] because the enzyme loading can be substantially increased and the diffusion resistance of substrates can be lowered significantly. Enzyme-immobilized nanofibrous membranes can also be applied to biosensor just by depositing nanofibers onto the electrode. Ren et al.[6] and Sawicka et al.[7] explored the application of electrospinning in glucose and urea biosensor, respectively, in which fast response and low detection limit were achieved. In their studies, enzyme was coelectrospun with water-soluble polymers followed by cross-linking. However, the swelling of water-soluble nanofibrous membranes by aqueous solutions should be avoided. This will prevent the leaching of enzymes from the nanofibers. On the other hand, the cross-linking agent should be carefully used because it may damage the active sites of enzymes. In consideration of reusability of the enzyme electrode, the use of water-insoluble nanofibrous membranes for the surface immobilization of enzymes would be a better alternative.

For an electrochemical biosensor, shortening the electron transfer distance between the deeply buried active site of electroactive protein and the electrode could enhance the current.[8] Carbon nanotubes (CNTs), discovered by Iijima,[9] have been attracting intensive attention because of their excellent properties such as superb electrical conductivity and remarkable mechanical strength and modules.[10,11] When explored as electrode materials, CNTs have shown efficient communications with redox proteins, including those where the redox center is embedded into the glycoprotein shell (e.g., glucose oxidase and microperoxidase).[12−15] In our previous work,[16,17] CNTs were filled into polyacrylonitrile-based nanofibrous membranes by electrospinning and it seemed to be a simple and effective approach for enhancing the activity of the immobilized redox enzymes. Therefore, when employing an electrospun nanofibrous membrane for enzyme electrode, CNTs filling is expected to increase the sensitivity potentially.

The glucose sensor has been drawing considerable attention because of its significance for diabetics.[18] Glucose oxidase (GOx) is commonly used as the biological element of the glucose sensor. In view of the advantage of electrospinning and CNTs in the electrochemical biosensor, in this work, a reactive-group-containing copolymer, poly(acrylonitrile-*co*-acrylic acid) (PANCAA), and a multiwalled carbon nanotube (MWCNT) were coelectrospun onto the Pt electrode, and then GOx was covalently immobilized onto the nanofibrous membrane (Figure 1). Our results indicate that MWCNT filling enhances the current of the GOx electrode obviously and moreover the electrodes show good reusability.

2. Experimental Methods

2.1. Materials. Poly(acrylonitrile-*co*-acrylic acid) (PANCAA) with a viscosity averaged molecular weight (M_v) of 8.32 × 10^4 g/mol was synthesized by a water phase precipitation

* Corresponding author. Fax: + 86-571-8795-1773. E-mail: xuzk@zju.edu.cn.
[†] Institute of Polymer Science and Key Laboratory of Macromolecular Synthesis and Functionalization (Ministry of Education).
[‡] State Key Laboratory of Industrial Control Technology, Institute of Advanced Process Control.

10.1021/jp807047s CCC: $40.75
Published on Web 01/23/2009

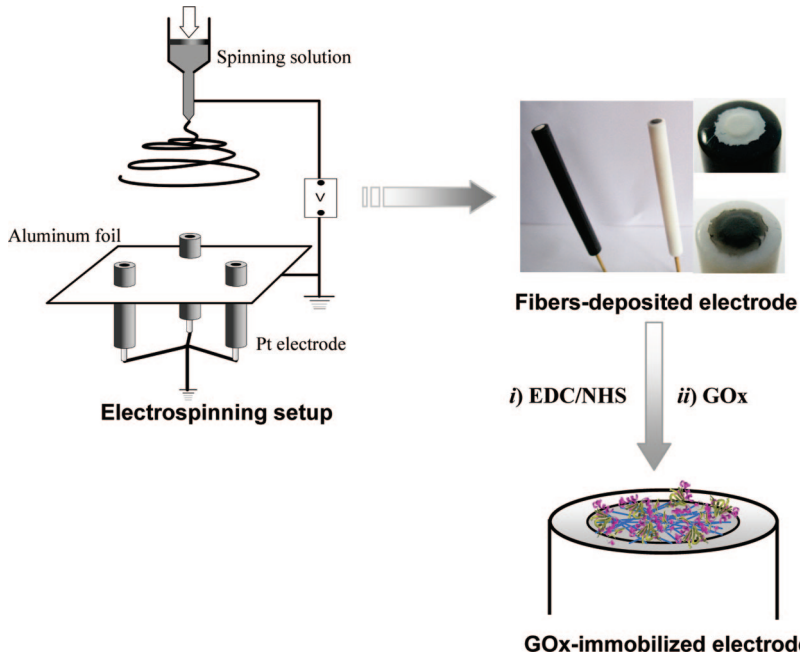

Figure 1. Schematic illustration of electrospinning for GOx electrode.

copolymerization process. The molar content of acrylic acid in this copolymer was about 10% by elemental analysis. GOx (EC 1.1.3.4, from *Aspergillus niger*) was purchased from Sigma. *N*-(3-Dimethylaminopropyl)-*N*′-ethylcarbodiimide hydrochloride (EDC) and *N*-hydroxysuccinimide (NHS) were HPLC grade and purchased from Shanghai Medpep (China). MWCNTs prepared by a chemical vapor deposition (CVD) process were purchased from Shenzhen Nanotech Port Co. Ltd. (China). Other reagents (e.g., D-glucose, *N*,*N*′-dimethylformamide, phosphate, and borate) were all analytical grade.

2.2. Preparation of Nanofibrous PANCAA/MWCNT Membranes by Electrospinning. To uniformly disperse MWCNT in the copolymer matrix, MWCNT was treated with a mixture of concentrated sulfuric and nitric acids (3:1, 98% and 70%, respectively) at 40 °C.[19] After chemical etching, the surface-oxidized MWCNT was well-dispersed in *N*,*N*′-dimethylformamide (DMF) after sonication for 10 h.

PANCAA was dissolved in the suspension of MWCNT in DMF at 100 °C. Its concentration was always kept at 5 wt %. The concentration of MWCNT was varied with 0%, 5%, 15%, and 25% of the mass of dissolved PANCAA. Electrospinning was carried out with use of a syringe with a 1.2 mm diameter stainless steel spinneret at an applied electrical potential difference of 14 kV over 15 cm gap between the spinneret and the Pt electrode surface. A microinfusion pump was set to deliver the solution at a feed rate of 1.0 mL/h with use of a 20 mL syringe. The electrospinning setup is schematically shown in Figure 1, in which the aluminum foil and Pt electrode were connected to the ground. Before electrospinning, the surface of the Pt electrode was polished thoroughly with 0.03 μm Al_2O_3 powder then rinsed with 5.0 wt % sulfuric acid and distilled water in turn. The ambient temperature and relative humidity for electrospinning were kept at 20−25 °C and 35−45%, respectively. It took 3−4 h to deposite the nanofibrous membranes on the surface of the Pt electrode.

2.3. Immobilization of GOx. GOx was covalently immobilized onto the nanofibrous membranes-deposited electrode with the EDC/NHS activation procedure. Briefly, the electrode surface was rinsed with borate−phosphate buffer solution (BPBS, 50 mM, pH 6.0) (*PBS mentioned in the following was the same unless otherwise specified*), submerged into an EDC/NHS solution (10 mg/mL in BPBS, the molar ratio of EDC to NHS = 1:1), and shaken gently for 2 h at 4 °C. The activated surface was taken out, washed several times with BPBS, and immersed into GOx solution (4.0 mg/mL in BPBS). GOx immobilization was conducted at 4 °C for 24 h. The resulting GOx-immobilized Pt electrode was thoroughly washed with BPBS.

2.4. Field Emission Scanning Electron Microscopy. Field emission scanning electron microscopy (FEI, SIRION-100, USA) was employed to evaluate the morphology of the PANCAA nanofibrous membranes. Before analysis, the samples were sputtered with gold with an Ion sputter JFC-1100.

2.5. Steady-State Fluorescence Spectroscopy. Steady-state fluorescence spectra were measured with a Hitachi F-4500 spectrofluorometer (Hitachi Co. Ltd., Japan). The samples for measurement were prepared by mixing MWCNTs with GOx in BPBS overnight. Final concentrations of MWCNT in GOx solution were 0, 10, 20, and 30 μg/mL, respectively. The concentration of GOx was 1.0 mg/mL of BPBS. The sample was excited at 285 and 450 nm, respectively, and the emission wavelength was set from 300 to 400 and 475 to 700 nm. The corresponding excitation/emission slit was set to 5.0/5.0 nm and 10.0/10.0 nm. The scanning speed was 100 nm/min.

2.6. Circular Dichroism (CD) Spectroscopy. CD measurements were performed on a Jasco J-815 circular dichroism spectrometer (Jasco Co. Ltd., Japan). The concentration of MWCNT was the same as in steady-state fluorescence assay and the concentration of GOx was 50 μg/mL in BPBS. The spectra were monitored in the near-UV region (190−250 nm) with a bandwidth of 2.0 nm and a scan speed of 200 nm/min. The CD spectrum of MWCNT (30 μg/mL) was recorded similarly as a control. The path length of the cell was 5 mm. Three scans were averaged. All CD measurements were performed at room temperature.

2.7. Electrochemical Measurements. A CHI760B electrochemical workstation (CHI instrument Inc., USA) was used for amperometric measurements. The GOx-immobilized Pt electrode was used as the working electrode, Ag/AgCl was used as the reference electrode, and a bare Pt electrode acted as the

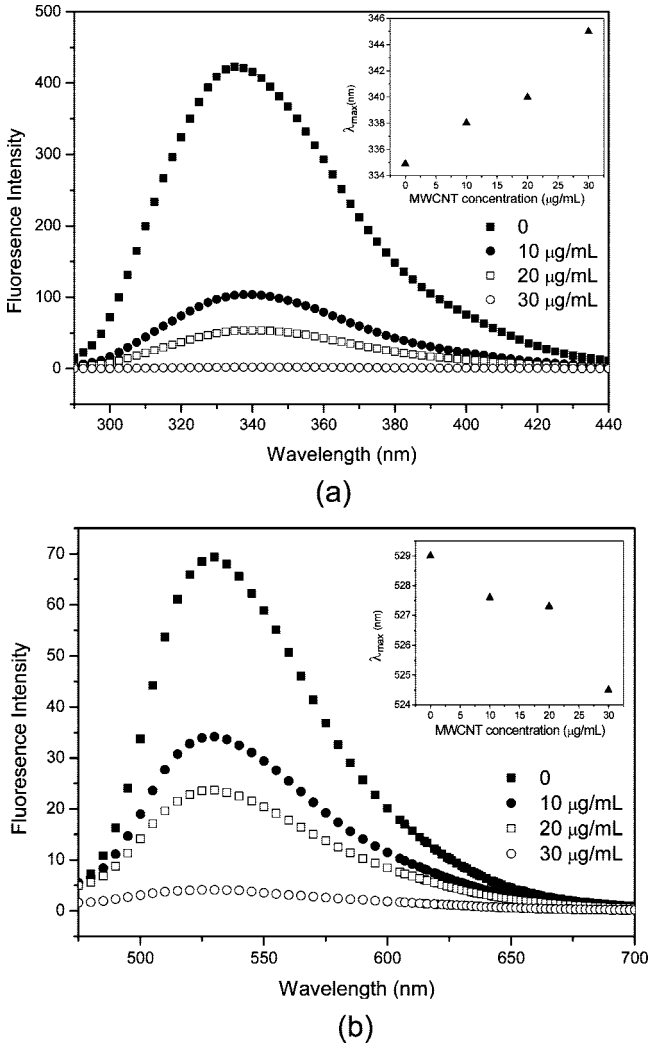

Figure 2. Fluorescence emission spectra of GOx. Excitation λ: (a) 285 and (b) 450 nm. The insets are the maximum fluorescence emission wavelengths of GOx at different MWCNT concentrations.

counter electrode. The working potential was +800 mV versus the Ag/AgCl reference electrode for glucose detection. When the electrode background current was stable, a designated amount of glucose was added into the reaction system and the current−time was recorded with an IBM PC compatible computer via a RS232 series port communicating to the electrochemical workstation. All measurements were performed in BPBS at 20 °C.

3. Results and Discussion

GOx is an enzyme with flavin adenine dinucleotide (FAD) as its active site, which is deeply embedded within a protective protein shell. The electron transfer distance between FAD and electrode surface is rather long due to the insulating shield of the protein shell.[8] Therefore, only if MWCNT penetrates inside the protein and gets close to FAD can electron transfer from FAD be promoted by MWCNT. Generally, variation in the structural characteristics of enzyme can be reflected by fluorescence and CD spectra,[20−22] which were herein used for evaluating the interactions between GOx and MWCNT.

Figure 2a shows the intrinsic fluorescence spectra of soluble GOx protein at different MWCNT concentrations. It can be seen that as the MWCNT concentration increases, the fluorescence intensity decreases obviously and the emission spectrum has

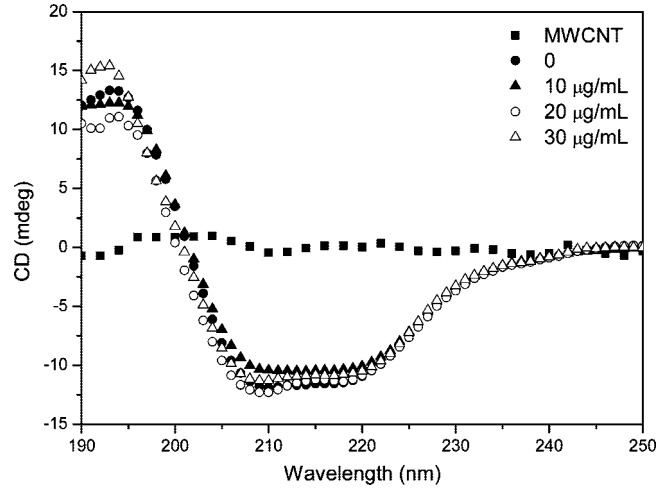

Figure 3. Far-UV CD spectra of GOx at different MWCNT concentrations.

TABLE 1: GOx Secondary Structure Percentage Calculated by Yang's Equation at Different Concentrations of MWCNT

MWCNT concn (μg/mL)	helix	beta	turn	random	total	rms value
0	14.3	65.1	4.5	16.1	100	13.993
10	13.6	66.7	3.3	16.4	100	20.983
20	12.5	64.0	3.5	20.0	100	14.912
30	11.7	63.8	5.0	19.5	100	15.284

an obvious red shift (335 to 345 nm). It is well-known that the fluorescence of a folded protein is a mixture of the fluorescence from individual aromatic residues (i.e., phenylalanine, tyrosine, and tryptophan).[23] However, as a result of resonance energy transfer (from proximal phenylalanine to tyrosine and from tyrosine to tryptophan) and the great difference in quantum yields and lifetimes, the fluorescence spectrum of a protein containing the three kinds of residues usually resembles that of tryptophan.[24,25] The polarity of the surroundings for the tryptophan residues can largely decide their fluorescence intensity and wavelength,[26] which in turn helps to determine the location of the tryptophan residues. In aqueous solution, when the tryptophan residues which are buried in the hydrophobic core turn over to the surface of the protein, the fluorescence intensity and peak tend to decrease and shift to a higher wavelength (red shift), respectively. It was usually seen as an unfolding process of the protein.[27,28] Therefore, the phenomena mentioned above demonstrate that MWCNT can induce GOx to unfold. On the other hand, the π-stacking interaction between the tryptophan residues and MWCNT can also result in the fluorescence quenching and red shift of the spectrum, since tryptophan is an electron donor[29,30] and MWCNT is known as an electron acceptor.[31,32]

CD spectra were used to assess the secondary structure of GOx for further study of the MWCNT−protein interactions. Typical spectra are shown in Figure 3, based on which secondary-structure calculations were carried out with the method described by Yang et al.[33] It can be seen from Table 1 that the secondary structure of GOx is impacted by MWCNT in an irregular way. In other words, after the addition of MWCNT into the GOx solution, the conformation of GOx is disturbed. This also indicates that the π-stacking interactions occur between MWCNT and the aromatic residues.

In GOx, FAD is surrounded by a number of amino acid residues, involving aromatic tyrosine (Tyr 68 and Tyr 515). Accordingly, the π-stacking interactions also provide the

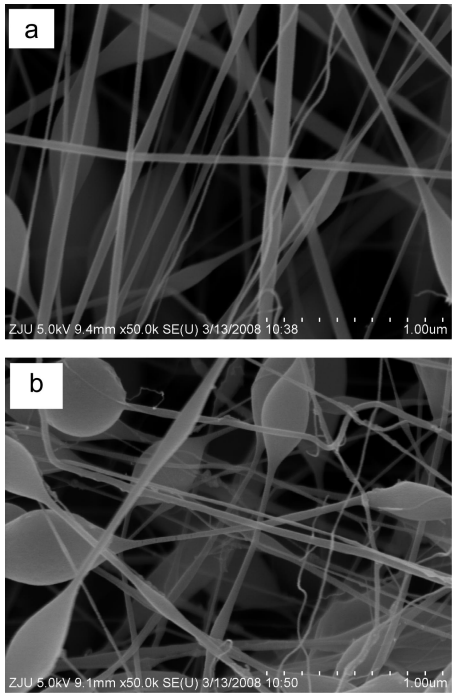

Figure 4. SEM images of electrospun PANCAA (a) and MWCNT-filled PANCAA (PANCAA/MWCNT) (b) nanofibrous membranes.

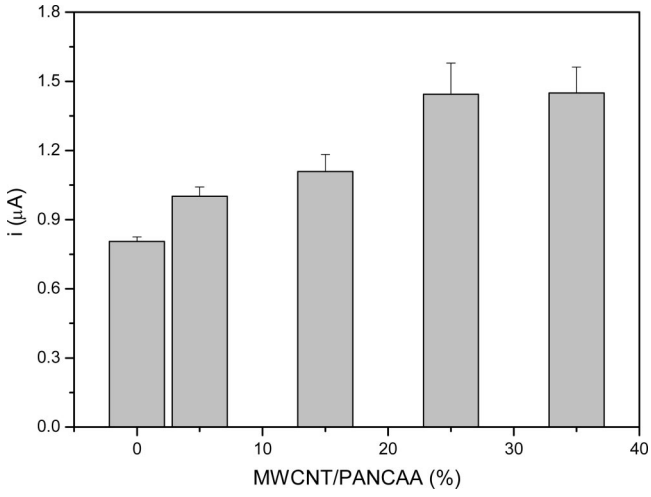

Figure 5. Effect of MWCNT/PANCAA mass ratio on the current of the GOx electrode.

possibility for MWCNT to approach FAD. On the other hand, flavin (chromophore of FAD) emits fluorescence when it is excited at 450 nm. Therefore, the fluorescence spectra can be used to monitor the surrounding change of FAD. Figure 2b shows that, as the MWCNT concentration increases, the fluorescence is quenched and the spectrum has a blue shift (529−524.5 nm), which indicates that the conjugation system of flavin is perturbed.[34] The perturbation of the conjugation system of flavin could be attributed to the conformational change of the protein, because as is known, flavin interacts with methionine (Met 561) and threonine (Thr 110) through hydrogen bonding in natural GOx. However, the irregular change of the secondary structure of GOx cannot result in the continuous blue shift of the FAD fluorescence spectrum. Therefore, it is likely that MWCNT gets close to flavin and perturbs the conjugation system. However, the mechanism of perturbation needs further study.

The structural characteristics of MWCNT and GOx ensure that MWCNT can interact with flavin when they are mixed in

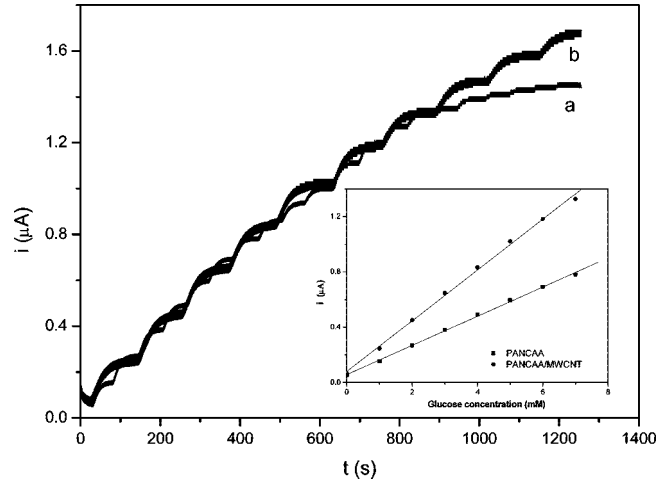

Figure 6. Chronoampeometric curves with various glucose concentrations (a) on the PANCAA nanofibrous membrane deposited electrode and (b) on the MWCNT-filled PANCAA (PANCAA/MWCNT) nanofibrous membrane deposited electrode. The glucose was added at every interval. The inset shows the plots of the steady-state limiting current against the concentration of glucose.

BPBS. GOx catalysis is a process of electron transfer through glucose, flavin, and oxygen (or electrode) in turn.[35] Such interaction will allow the promotion of electron transfer by MWCNT during GOx catalysis. Therefore, in this study, MWCNT was filled into the PANCAA nanofibrous membranes by electrospinning for GOx immobilization. The MWCNT-filled nanofibrous membranes provide several advantages for glucose biosensor. First, the membranes possess reactive groups for the covalent immobilization of GOx. Second, the large specific surface area and high porosity will favor the GOx immobilization and glucose diffusion. Third, MWCNT usually protrudes out of the nanofibers (as seen from our previous study[17]) and will interact with GOx. Forth, the nitrile groups in PANCAA can form charge-transfer complexes with MWCNT and the electrical conductivity will be enhanced up to several orders.[36] Fifth, the water-insoluble property of the PANCAA nanofibrous membrane will allow the GOx electrode to be reusable.

As shown in Figure 1, the nanofibrous membranes were deposited onto the Pt surface of the electrode by using the special electrospinning setup. Then GOx was directly immobilized onto the membrane through EDC/NHS activation. Figure 4 shows the images of the nascent PANCAA and the MWCNT-filled PANCAA nanofibrous membranes, which are interspersed with beads. It is found that the composite membrane has more beads than the nascent PACAA membrane. The beads were very common nanofiber defects. Their formation might be because of the change of the spinning solution properties and the low relative humidity of the surroundings.[37] According to our previous study,[38] MWCNT filling only has a small effect on the enzyme loading. Therefore, to eliminate the effect of GOx loading on the electrode current, similar amounts of membrane (~0.20 mg) were prepared by controlling the electrospinning time.

The effect of MWCNT/PANCAA mass ratio on the electrode current is shown in Figure 5. A glucose concentration of 5 mM was selected for the measurements. It can be seen that the current increases until the ratio raises to 25 wt %. This can be attributed to the formation of percolating network among MWCNTs[36] and to much more MWCNT protruded out of the nanofiber, which enhances the electrical conductivity of the nanofibrous membrane and increases the opportunity for GOx to interact with

TABLE 2: Parameters for GOx-Immobilized Electrode

sample	sensitivity ($\mu A \cdot mM^{-1}$)	detection limit (mM)	response time (s)	K_m (mM)	I_{max} (μA)
PANCAA nanofibrous membrane	0.10543	0.557	20	12.13	1.99
MWCNT-filled PANCAA nanofibrous membrane	0.18354	0.668	35	17.54	4.46

MWCNT. However, the current changes little as the MWCNT/PANCAA mass ratio increases from 25 to 35 wt %. Furthermore, the nanofibrous membrane with a MWCNT/PANCAA mass ratio of 35 wt % easily detaches from the electrode during the current measurement.

To examine the electrochemical properties of the GOx electrode, measurements were carried out to plot the typical amperometric current−time response curves through successive aliquot addition of glucose to BPBS (Figure 6). Herein, the PANCAA and the MWCNT-filled PANCAA (MWCNT/PANCAA mass ratio: 25 wt %) nanofibrous membranes were selected as supports for GOx immobilization, respectively. It is found from the calibration curves that the response current is linear with the glucose concentration from 0 to 7 mM for both electrodes. The parameters of the electrodes, obtained from Figure 6, are indicated in Table 2. The sensitivity was calculated according to the calibration curves (inset of Figure 6). The kinetic parameters (i.e., apparent Michaelis−Menten constant K_m^{app} and maximum current I_{max}) were determined by a double reciprocal plot (Lineweaver−Burk method). It can be seen from Table 2 that MWCNT filling increases the sensitivity and I_{max} as well as K_m^{app} obviously, while the response of the electrode is delayed. Table 2 also shows that the detection limit is raised by MWCNT filling. The detection limit is defined to be three times the noise. MWCNTs filling can enhance electrical conductivity of the nanofibers, which also contributes to the increase of the background current and the noise.

The increase of the sensitivity and I_{max} indicates clearly that MWCNT filling enhances the activity of the immobilized GOx. However, the response of the electrode is limited by the diffusion of H_2O_2. In other words, GOx on the MWCNT-filled PANCAA nanofibrous membranes can catalyze the reduction of O_2 (or oxidation of glucose) to generate more H_2O_2, while the H_2O_2 molecules are subject to more hindrance when diffusing through the MWCNT-filled PANCAA nanofibrous membrane toward the electrode surface. The increase of K_m^{app} reflects the lower possibility of forming a glucose−GOx complex and is indicative of the undesirable conformational change of GOx. It decreases the activity of enzyme, which is contradictive to the above results. Therefore, it can be further concluded that the interaction of MWCNT with flavin of GOx plays a significant role in promoting the catalytic activity of the immobilized GOx.

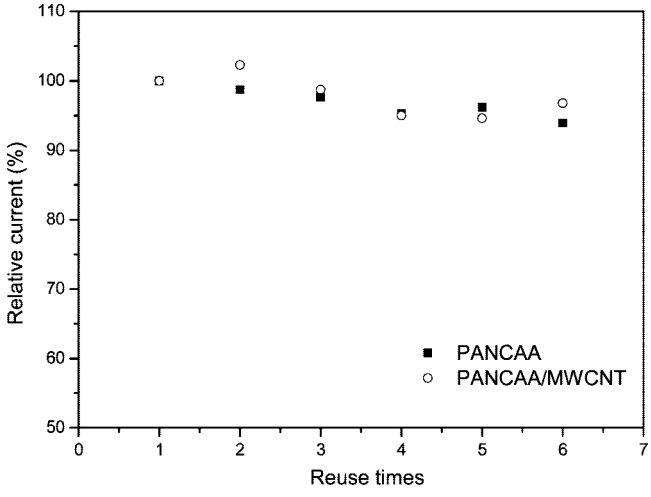

Figure 7. Reusability of the GOx electrodes.

The reuse stability of the electrodes was also studied. It is a very important parameter for enzyme electrodes. However, this parameter was often ignored in previous studies on the electrochemical biosensor. It is probably because most of the studied enzyme-immobilized carriers were highly hydrophilic or water-soluble materials (e.g., PPy,[39] CNTs,[40] PVP[13]). In our case, water-insoluble nanofibrous membranes were used instead and enzyme was covalently immobilized onto the membranes. From Figure 7, it can be seen that the electrodes can be used at least 6 times, and MWCNT filling has little effect on the reusability. The significant reduction in current after 6 uses is due to the detachment of the membrane from the electrode. Therefore, it is necessary to enhance the interfacial adhesion between the nanofibrous membrane and the electrode for further improving the reusability.

4. Conclusion

In summary, this work applied electrospun MWCNT-filled nanofibrous membranes for use as glucose biosensors. The reactive groups possessed by the membranes were used for the covalent immobilization of GOx. It seems that MWCNT could approach FAD, the active site of GOx, and disturbs the enzyme conformation. It suggests preliminarily that during the catalysis of GOx, the electron has the potential to transfer through MWCNT from FAD. The results from chronoamperometric measurements show that MWCNT filling enhances the electrode current and sensitivity obviously. Combined with the results of kinetic studies, we conclude that the interactions between MWCNT and FAD play a significant role in enhancing the electroactivity of the immobilized GOx. Moreover, the electrodes show a good reusability.

This work provides a simple method to enhance the current and to improve the reusability of the enzyme electrode. However, several problems are still left to resolve. First, although MWCNT filling increases the current, the response is delayed at the same time. Therefore, shortening the response time will be urged if the electrode studied is chosen for diagnostic applications. Second, the interface adhesion between nanofibrous membrane and the electrode is still expected to be enhanced for better reusability. Third, although it has been demonstrated from the spectra that MWCNT could approach the active site of soluble GOx, the mechanism of enhanced electron transfer for the GOx electrode is just based on hypothesis. Therefore, clarifying the interactions of embedded MWCNT with immobilized GOx will be necessary in future study.

Acknowledgment. Financial support from the National Natural Science Foundation of China for Distinguished Young Scholars (Grant no. 50625309) is gratefully acknowledged.

References and Notes

(1) Li, D.; Xia, Y. N. *Adv. Mater.* **2004**, *16*, 1151–1170.
(2) Reneker, D. H.; Chun, I. *Nanotechnology* **1996**, *7*, 216–223.

(3) Wu, L. L.; Yuan, X. Y.; Sheng, J. *J. Membr. Sci.* **2005**, *250*, 167–173.
(4) Jia, H. F.; Zhu, G. Y.; Vugrinovich, B.; Kataphinan, W.; Reneker, D. H.; Wang, P. *Biotechnol. Prog.* **2002**, *18*, 1027–1032.
(5) Nair, S.; Kim, J.; Crawford, B.; Kim, S. H. *Biomacromolecules* **2007**, *8*, 1266–1270.
(6) Ren, G. L.; Xu, X. H.; Liu, Q.; Cheng, J.; Yuan, X. Y.; Wu, L. L.; Wan, Y. Z. *React. Funct. Polym.* **2006**, *66*, 1559–1564.
(7) Sawicka, K.; Gouma, P.; Simon, S. *Sens. Actuator, B* **2005**, *108*, 585–588.
(8) Habermuller, L.; Mosbach, M.; Schuhmann, W. *Fresenius' J. Anal. Chem.* **2000**, *366*, 560–568.
(9) Iijima, S. *Nature* **1991**, *354*, 56–58.
(10) Rao, C. N. R.; Satishkumar, B. C.; Govindaraj, A.; Nath, M. *ChemPhysChem* **2001**, *2*, 78–105.
(11) Wang, J. *Electroanalysis* **2005**, *17*, 7–14.
(12) Guiseppi-Elie, A.; Lei, C. H.; Baughman, R. H. *Nanotechnology* **2002**, *13*, 559–564.
(13) Joshi, P. P.; Merchant, S. A.; Wang, Y. D.; Schmidtke, D. W. *Anal. Chem.* **2005**, *77*, 3183–3188.
(14) Davis, J. J.; Coleman, K. S.; Azamian, B. R.; Bagshaw, C. B.; Green, M. L. H. *Chem.*−*Eur. J.* **2003**, *9*, 3732–3739.
(15) Gooding, J. J.; Wibowo, R.; Liu, J. Q.; Yang, W. R.; Losic, D.; Orbons, S.; Mearns, F. J.; Shapter, J. G.; Hibbert, D. B. *J. Am. Chem. Soc.* **2003**, *125*, 9006–9007.
(16) Wan, L. S.; Ke, B. B.; Wu, J.; Xu, Z. K. *J. Phys. Chem. C* **2007**, *111*, 14091–14097.
(17) Wang, Z. G.; Ke, B. B.; Xu, Z. K. *Biotechnol. Bioeng.* **2007**, *97*, 708–720.
(18) Abel, P. U.; von Woedtke, T. *Biosens. Bioelectron.* **2002**, *17*, 1059–1070.
(19) Liu, J.; Rinzler, A. G.; Dai, H. J.; Hafner, J. H.; Bradley, R. K.; Boul, P. J.; Lu, A.; Iverson, T.; Shelimov, K.; Huffman, C. B.; Rodriguez-Macias, F.; Shon, Y. S.; Lee, T. R.; Colbert, D. T.; Smalley, R. E. *Science* **1998**, *280*, 1253–1256.
(20) Chattopadhyay, K.; Mazumdar, S. *Biochemistry* **2000**, *39*, 263–270.
(21) Mu, Q. X.; Liu, W.; Xing, Y. H.; Zhou, H. Y.; Li, Z. W.; Zhang, Y.; Ji, L. H.; Wang, F.; Si, Z. K.; Zhang, B.; Yan, B. *J. Phys. Chem. C* **2008**, *112*, 3300–3307.
(22) Asuri, P.; Bale, S. S.; Pangule, R. C.; Shah, D. A.; Kane, R. S.; Dordick, J. S. *Langmuir* **2007**, *23*, 12318–12321.
(23) Steiner, R. F.; Edelhoch, H. *Chem. Rev.* **1962**, *62*, 457–483.
(24) Liang, J. N.; Chakrabarti, B. *Biochemistry* **1982**, *21*, 1847–1852.
(25) Bizzozero, O. A.; Lees, M. B. *Biochemistry* **1986**, *25*, 6762–6768.
(26) Itzhaki, L. S.; Evans, P. A.; Dobson, C. M.; Radford, S. E. *Biochemistry* **1994**, *1994*, 5212–5220.
(27) Duy, C.; Fitter, J. *Biophys. J.* **2006**, *90*, 3704–3711.
(28) Monteiro, R. Q.; Foguel, D.; Castro, H. C.; Zingali, R. B. *Biochemistry* **2003**, *42*, 509–515.
(29) Froehlich, P. M.; Nelson, K. *J. Phys. Chem.* **1978**, *82*, 2401–2403.
(30) de Visser, S. P.; Shaik, S.; Sharma, P. K.; Kumar, D.; Thiel, W. *J. Am. Chem. Soc.* **2003**, *125*, 15779–15788.
(31) Baskaran, D.; Mays, J. W.; Zhang, X. P.; Bratcher, M. S. *J. Am. Chem. Soc.* **2005**, *127*, 6916–6917.
(32) Guldi, D. M.; Rahman, G. M. A.; Zerbetto, F.; Prato, M. *Acc. Chem. Res.* **2005**, *38*, 871–878.
(33) Yang, J. T.; Wu, C. S. C.; Martinez, H. M. *Methods Enzymol.* **1986**, *130*, 208–269.
(34) Kim, J.; Swager, T. M. *Nature* **2001**, *411*, 1030–1034.
(35) Wohlfahrt, G.; Witt, S.; Hendle, J.; Schomburg, D.; Kalisz, H. M.; Hecht, H. J. *Acta Crystallogr. D* **1999**, *55*, 969–977.
(36) Ge, J. J.; Hou, H. Q.; Li, Q.; Graham, M. J.; Greiner, A.; Reneker, D. H.; Harris, F. W.; Cheng, S. Z. D. *J. Am. Chem. Soc.* **2004**, *126*, 15754–15761.
(37) Greiner, A.; Wendorff, J. H. *Angew. Chem., Int. Ed.* **2007**, *46*, 5670–5703.
(38) Wang, Z. G.; Xu, Z. K.; Wan, L. S.; Wu, J.; Innocent, C.; Seta, P. *Macromol. Rapid Commun.* **2006**, *27*, 516–521.
(39) Wang, J.; Musameh, M. *Anal. Chim. Acta* **2005**, *539*, 209–213.
(40) Sotiropoulou, S.; Chaniotakis, N. A. *Anal. Bioanal. Chem.* **2003**, *375*, 103–105.

JP807047S